



Using geostatistical modeling methods to assess concentration and spatial variability of trace metals in soils of the abandoned gold mining district of Bindiba (East Cameroon)

Martin Mozer Njayou¹ · Mouhamed Ngounouno Ayiwou² · Luc Leroy Ngueyep Mambou^{2,3} · Ismaïla Ngounouno⁴

Received: 6 September 2022 / Accepted: 1 October 2022 / Published online: 20 October 2022
© The Author(s), under exclusive licence to Springer Nature Switzerland AG 2022

Abstract

Trace metal pollution in surface soils is of special concern given the potential dangers to human health. This paper uses geostatistical modelling to assess the spatial variability of soil physico-chemical parameters (pH, EC) and trace metals (Cr, Ni, Cu, As and Pb) in the abandoned gold mining district of Bindiba (East Cameroon). Two sampling campaigns are carried out in the dry season and rainy season and a total of 89 samples are collected at an average spacing of 50 m. To produce realistic prediction maps at un-sampled locations, geostatistical analysis is used. The geostatistical approach use exploratory analysis, variographic analysis (VA), and ordinary kriging (OK). The soils of the abandoned gold mining district are characterized by acidic to near neutral pH (5.01–6.19), weakly conductivities (7–47 $\mu\text{S cm}^{-1}$) and trace metals range from Pb (0.006–53.27 mg kg^{-1}), As (0.00–46.58 mg kg^{-1}), Cr (22.15–442.44 mg kg^{-1}), Ni (9.25–360.37 mg kg^{-1}) and Cu (1.28–320.86 mg kg^{-1}). The variographic analysis of pH, EC and trace metals which highlight the heterogeneity of the contamination, reveal two variogram models, spherical model for Cr, As, Pb, pH and EC, and exponential model for Ni and Cu. The trace metals Pb (1.95) and As (1.78) show the highest variability, while the lowest variability is observed for Cu (0.37). The length of the spatial autocorrelation is much longer than the sampling step indicating that the sampling design adopted in this study is appropriate. The nugget/sill ratio values of 0.65, 0.67, 0.62, 0.27, 0.57 and 0.19 for pH, EC, Cr, Ni, As and Pb, respectively, suggest a moderate spatial dependence. High concentrations of potentially toxic elements are found in the soils of the study area, indicating that anthropogenic factors are causing the anomalies in these areas. The maps obtained from the geostatistical modelling accurately described the spatial variability of trace metal concentrations in soil. Thus, this study could help decision makers to develop a better soil management strategy.

Keywords Abandoned gold mining · Soils · Trace metals contamination · Spatial variability · Cross validation · Geostatistical modeling

Introduction

The exploitation of mining sites has become over time a very important economic activity as the industrialization of companies has taken place. With a continuous increase in the demand for metals, mining activity has begun to affect the environment more seriously; with great changes in the landscape and the volumes of rocks, it concerns (Alloway and Ayres 1997; Custer 2003).

Trace metal contamination of soils is a hazard to water, living species and human health. Trace metal concentrations (TMs) are related to the nature of the parent rock and to weathering processes (Baize 2009). According to Dère (2006), the migration of TMs is controlled by several factors: the metal itself, the physico-chemical characteristics of

✉ Martin Mozer Njayou
njayoumozer@gmail.com

¹ Department of Mining and Geology, School of Geology and Mining Engineering, University of Ngaoundere, P.O. Box 115, Meiganga, Cameroon

² Department of Mining Engineering, School of Geology and Mining Engineering, University of Ngaoundere, P.O. Box 115, Meiganga, Cameroon

³ Laboratory of Material Sciences, Department of Physics, Faculty of Sciences, University of Yaoundé 1, P.O. Box 812, Yaoundé, Cameroon

⁴ Department of Earth Sciences, Faculty of Sciences, University of Ngaoundere, P.O. Box 454, Ngaoundere, Cameroon

the soil (pH and EC), the intrinsic properties of each horizon (texture, structure, cohesion, etc.), the water flows and their dynamics. Therefore, high levels of trace metal concentrations can be found after migration around metal mines due to the dumping and dispersion of mine waste in the surrounding soils, crops and rivers. They may eventually pose a potential health risk to residents near mining areas (Jung 2001). Trace metals are bio-persistent, disrupt ecosystems, deteriorate soils, surface waters, forests, crops and accumulate in the food chain (Gouzy and Ducos 2008; Jaishankar et al. 2014).

The objective of mining is the extraction of materials consisting of a set of minerals: ores. But this extraction is associated with other activities such as the processing of minerals leading to the production of tailings. It is these tailings that, initially in geochemical equilibrium at depth, are exposed to a new environment, namely the soil, surface water and air. Contact with surface water, which is often less ionically charged, can have an impact on the balance of dissolution and precipitation (Sigg et al. 1992). The oxidation of sulphides causes extreme acidification of the environment and thus of the leach water from these tailings: this is the typical Acid Mine Drainage (AMD) of mine tailings (Edraki et al. 2005; Lottermoser and Ashley, 2005). His acidification has important consequences since it favours the desorption of certain heavy metals or metalloids (Chromium, Copper, Nickel, Arsenic, Lead, etc.) in more mobile and toxic forms, and produces highly polluted water which in turn affects the soil.

Geostatistical analysis consists of predicting an unknown variable using a property measured at a given position and time (Yasrebi et al. 2009). Geostatistics allows for consistent analysis of data, uncertainties and errors in the data, and spatial structuring of grades (Malherbe and Rouil 2003). This analysis in turn allows the production of concentration maps of the studied parameters (Florine et al. 2019). Based on the assumption of estimating an unknown variable at any position, several techniques have been developed to predict the spatial variability of soil properties, such as ordinary kriging (OK), inverse distance weighting (IDW), artificial neural networks and soil transfer functions (Zhao et al. 2010; Veronesi et al., 2014). In recent years, OK has been widely used by many authors for the preparation of spatial variability maps of trace metals and soil physicochemical parameters (Behera et al. 2016; Behera and Shukla 2015; Tripathi et al. 2015). In practice, the first step is to carry out an exploratory analysis of the data (location map, descriptive statistics, histogram, etc.) in order to identify general trends, anomalous data and delineate areas with different properties (GeoSiPol 2005; Mathieu et al. 2014). The next step, which consists of characterizing the spatial variability of the physicochemical properties of the soils, in

particular the extent or correlation distance and the anisotropy of the environment, helps to guide the choice of the interpolation method. The geostatistical approach used to map the physicochemical parameters (pH and EC) and the trace metals (Cr, Ni, Cu, As and Pb) spatial variabilities, in this study includes four phases: effective analysis of the data, which consists of determining the statistical characteristics necessary to describe the pollution of the soils; interpolation of the levels of pollutants by the kriging method based on realistic maps of the spatial dispersion of pollutants in soils; estimation of contaminated areas and determination of critical thresholds. Geostatistical approach appears as an effective tool to help managers of polluted sites and soils in possible clean-up projects (Deraisme and Bobbia 2003; GeoSiPol 2005; Jeannée and De Fouquet 2000; Jeannée, 2005; Kumar et al. 2016).

The study of spatial variability of physico-chemical parameters (pH and EC) and trace metals (Cr, Ni, Cu, As and Pb) of a former site requires the creation of pollutant concentration maps at the level of the study area (Bhunias et al. 2018; Khan et al. 2019). It is necessary to spatialise the pollutant levels obtained at a few sampling points on the site, thanks to laboratory analyses carried out after a rigorous sampling campaign. Several authors (Leenaers et al. 1989; Scholz et al. 1999; Jeannée and De Fouquet 2003; Demougeot et al. 2009; Garcia et al. 2019) have used geostatistical techniques in the study of soil quality to map and estimate the concentrations of pollutants present at the site and regional scale. The geostatistical approach also makes it possible to integrate other information relevant to the mapping of the pollutant: concentrations from physicochemical modelling, land use, and measurements of other pollutants with similar behaviour (Bobbia et al. 2001).

Numerous studies have evaluated soil pollution using traditional methods. These approaches include: quality guidelines (SQGs), statistical multivariate techniques, calculated pollution indices and/or ecological risk assessments (Ayiwou et al. 2022; Chen et al. 2021).

In the present study, a site sensitivity analysis demonstrates the value of in-depth geostatistical modeling. This modeling entails a thorough exploratory data examination, which is necessary for any estimating technique. In order to account for the heterogeneity of the distribution of the concentrations on the site, the aim is to detect the spatial variability of the concentrations and quantify it using a variogram. The various variogram models necessary for simple kriging interpolation are chosen using the cross-validation technique.

The main objective of this study is to assess the spatial variability of physico-chemical parameters (pH and EC) and trace metals (Cr, Ni, Cu, As and Pb) in the abandoned gold mining district of Bindiba (East Cameroon) and to predict their values at unsampled locations.

Materials and methods

Study area, sampling and analytical procedures

The study area is located about 12 km from the locality of Bindiba, in the district of Garoua-Boulai, Lom and Djerem department, East Region of Cameroon (Fig. 1). It covers an area of about 3092.34 km². The study area has an equatorial Guinean climate. With around 2.1 months of extreme heat and four months of extreme cold, there are four seasons of differing lengths (PCD, 2012). The temperature ranges from 14 to 35 °C all year long. The South Cameroon plateau, which has an altitude range of 650–900 m, accounts for the majority of the relief in the Eastern Region of Cameroon (PCD 2012). Although gold mining has significant economic benefits, it also degrades the quality of the local soils, which leads to the unregulated dumping of mining waste on the site, which has a significant negative impact on the ecosystem.

The sampling map is presented in Fig. 1.

It was vital to optimize sampling and analysis to assure the quality of the data, so the sample sites were chosen based on the mining density. During the course of this study's first site reconnaissance, acid mine drainage was discovered at a few different locations on the site. Thus, there were two soil sampling campaigns. The first was conducted during the rainy season, specifically in August 2020, and resulted in the collection of 33 samples. During this campaign, sampling was done at intervals that were, on average, 100 m apart. In May 2021, a total of 56 samples were collected with an average spacing of 50 m as part of the second campaign, which intended to enhance sampling density. The differences in pitch between the two sample campaigns are caused by the anthropogenic (houses, deep trenches, lakes, embankments, etc.) and natural (vegetation, mountains, rivers, etc.) obstructions present in the study area. To prevent the sample technique from affecting the statistics, all these step changes were implemented. A total of 89 soil samples were collected during the study (Fig. 1).

As recommended by IAEA (2004), a systematic sampling was used as the sampling strategy since it enables for the determination of average pollutant concentrations as well

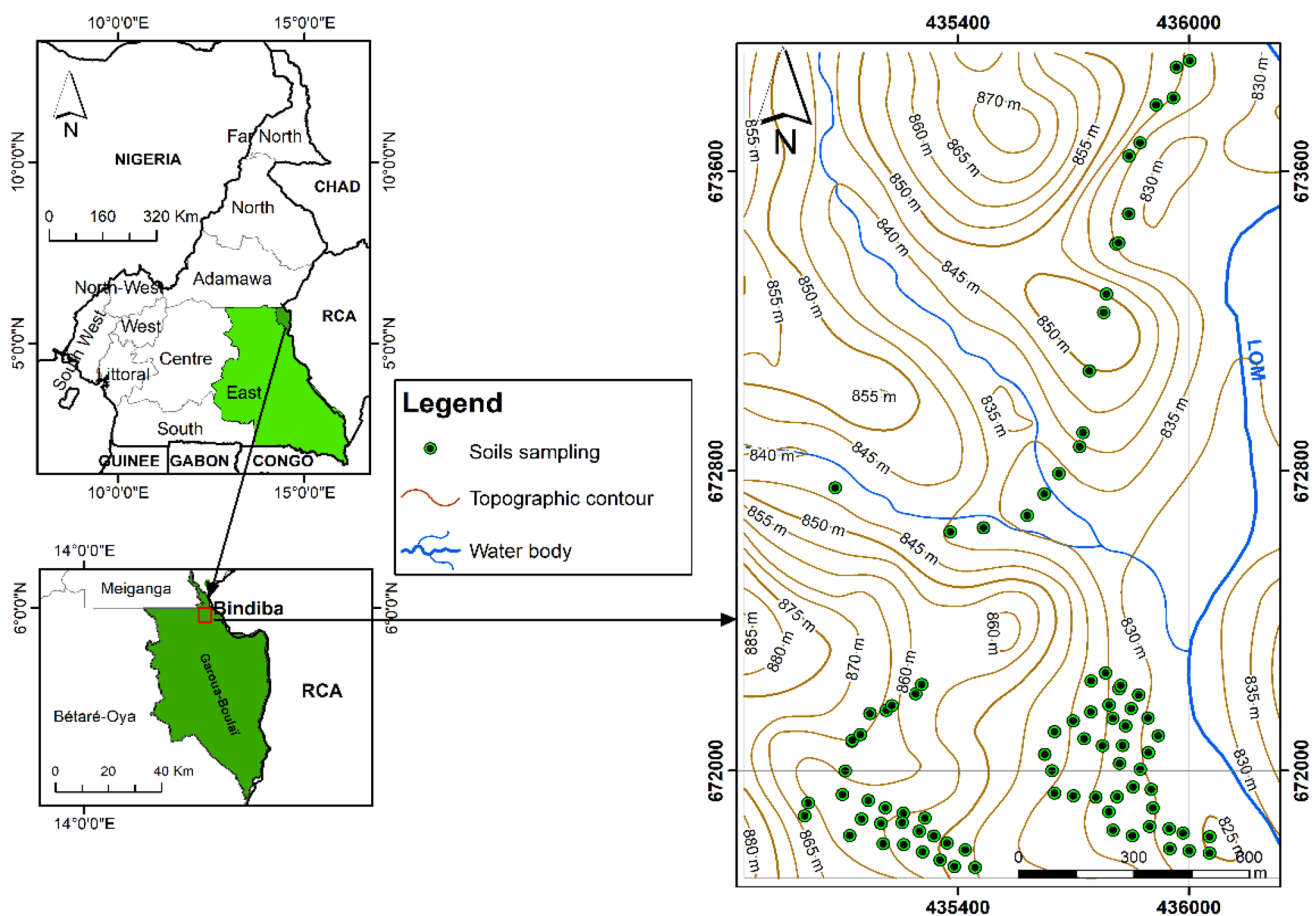


Fig. 1 Map of the study area and locations of the sampling sites

as the parameters pH and EC in various cells. A volume of 500 g per sample was collected, preserved in polythene bags, and brought to the lab for additional examination after samples were manually taken at depths ranging from 0 to 10 cm.

The analysis of the physico-chemical parameters consisted in determining the pH and EC using a pH meter and a multi-parameter apparatus of the brand HANNA HI991300-HI991301 previously calibrated. The method consisted of introducing the sediment sample (6 ± 1 g) into a jar containing distilled water (15 mL) (AFNOR NF X-31-103, 1998). The sample was then stirred in the jar for 20 min and then left to stand for the decantation of the solid elements for 30 min. After complete settling, pH and EC measurements were taken. For each sample, the electrode was rinsed with distilled water and dried, then the operation was repeated for each sample. The pH and EC were analyzed at the Laboratory of Environment and Eco-materials of the School of Geology and Mining Engineering of the University of Ngaoundéré, Cameroon.

The trace metals analyzed in the soil samples were chromium (Cr), nickel (Ni), copper (Cu), arsenic (As), and lead (Pb). Their concentrations were determined in mg kg^{-1} using the Skyray Instrument EDX Pocket III X-ray fluorescence spectrometer with a detection limit of 0.001–0.01%. The analysis was carried out at the laboratory of the Framework of Support for the Promotion of Mining Handicrafts “(CAPAM)” located in Yaounde, Cameroon.

Geostatistical analysis

The geostatistical analysis consisted in three steps. The first step was the exploratory analysis of data, the second was the variographic analysis (VA) and the third, production of prediction maps with kriging interpolation (Chiles et al. 2009).

Exploratory analysis

The base of any geostatistical analysis is the exploratory data analysis (Rivoirard 2003). It is a crucial phase in comprehending a dataset and enables first-class information base cleaning (positioning, copying errors, etc.), followed by the development of each quantity's primary statistical characteristics as well as the connections between them.

The exploratory analysis, which follows the numerous sampling phases with their flaws and faults, entails a statistical study of the concentrations of the pollutants being tracked, including correlations between various elements and the statistical distribution of concentrations. By characterizing the histograms, it is possible to identify outliers or suspicious values at this phase. Additionally, it enables the visualization of the distribution curve and perhaps the detection of many modes. We can choose the best interpolation approach by using the exploratory analysis to better understand the spatial

organization of the information (Jeannée and De Fouquet 2003).

Variographic analysis

The variogram (or semi-variogram) is a geostatistical tool that allows the quantification of spatial variability as a function of distance. It is defined experimentally as the average over the field studied of the half-square of the difference between the values measured at two points, as a function of the distance and orientation separating these two points. A variogram (or semi-variogram) is used to measure the spatial variability of a regionalised variable and provides the input parameters for spatial interpolation of the kriging (Webster and Olivier 2006). It can be expressed as follows.

$$\gamma(h) = \frac{1}{2N(h)} \sum_{i=1}^{N(h)} N(h)[Z(x_i + h) - Z(x_i)]^2 \quad (1)$$

where $N(h)$ is the number of pairs of points distant from h ; $[Z(x_i + h) - Z(x_i)]^2$ the squared deviation of the contents at points x and $x + h$.

The VA is the first step for obtaining the kriging weights λ_i . The so-called semivariogram $\gamma(h)$ represents the average variance between the observations separated by a certain distance, and describes the structure of the spatial variability of the investigated variable (Chambers et al. 2000). The semivariogram is calculated by using Eq. (2) (Journel and Huijbregts 1978):

$$\gamma(h) = \frac{1}{2N(h)} \sum_{i=1}^{N(h)} (Z(x_i + h) - Z(x_i))^2, \quad (2)$$

where N is the number of pairs of sample points separated by the distance h .

The semivariogram, however, often does not provide information for all possible distances. Therefore, a semivariance model must be fitted to the semivariogram (such as a stable, exponential, or spherical model). The type of model is selected based on the properties of the data. We basically follow the rule that the sum of the products of the lag size and the number of lags in the semivariogram should be approximately half the distance between all points (Verfaillie et al. 2006).

In geostatistical modeling, sampled data are considered as the result of a random process. Therefore, there is always some likelihood or uncertainty attached to the predictions. In order to do this, the Kriging system is defined by Eq. (3):

$$\hat{Z}_1(S_0) = \mu_1 + \varepsilon_1(S_0), \quad (3)$$

where \hat{Z}_1 is the estimated variable at location S_0 decomposed into the deterministic trend μ_1 and the random, auto-correlated error ε_1 at location S_0 .

The best-fitting model was selected for each soil parameter with root mean square error (RMSE).

$$RMSE = \sqrt{\frac{1}{N} \sum_{i=1}^N [Z(x_i) - \bar{Z}(x_i)]^2} \tag{4}$$

where $Z(x_i)$ is the predicted value from cross-validation; $\bar{Z}(x_i)$ the observed value.

Interpolation by the kriging method

As the most precise spatial interpolation technique from a statistical standpoint, kriging enables a linear estimation based on statistical quantities of spatialized data (Baillargeon 2005). It is a single-variable geostatistical method that minimizes the estimation variance determined using the variogram while computing, interpreting, and modeling the variance as a function of the distance between the data. Kriging, in contrast to other methods, is preceded by an investigation of the spatial variability of trace metal concentrations and physicochemical properties at the site and is followed by a computation of the related estimate's error (Wu et al. 2010). The estimated concentration z of a given pollutant at a point x_0 , denoted $Z^*(x_0)$ is obtained by linear combination of n concentrations at the measurement points:

$$Z^*(x_0) = \sum_{i=1}^n \lambda_i Z^*(x_i). \tag{5}$$

The choice of coefficients λ_i called kriging weights makes it possible to differentiate kriging interpolation from other classical interpolation techniques (inverse of distances, nearest neighbour, etc.). λ_i depends on the distances between the data and the target x_0 , the distances separating the data from each other (taking into account the grouping of data, in particular at the operation site) and the spatial variability of the soil parameters.

The ordinary kriging, which is appropriate for the analysis of polluted sites and soils (Khan et al. 2019; Gaida et al. 2019), was used to create the prediction maps while also taking into account the spatial variability of the studied parameters. These maps offer helpful visual representations of spatial variability in the field and can be used to summarize and portray soil characteristics where it is possible to identify natural hazards (Goodchild et al. 1993). Any interpolated map can be matched with a precision map using this estimator. ISATIS-neo software was utilized to carry out the geostatistical study.

Accuracy assessment

The effectiveness of spatial variability maps has been evaluated using the cross-validation method (Delfiner 1976; Parker et al. 1979; David 1987). This method entails eliminating the data one at a time, then estimating the remaining data by kriging from the deleted ones (Chilès and Delfiner 1999). It also enables the evaluation of the magnitude of the point estimate's mistakes. The selection of the various models in this study was made following the cross-validation procedure. For this, three evaluation indices were used: the mean absolute error (MAE) and the root mean square error (MSE) measure the accuracy of the prediction, while the prediction quality (G) measures the effectiveness of the prediction (Utset et al. 2000). The experimental histogram of standardised errors (error divided by the standard deviation of the kriging) can be used to validate the assumption of normality of estimation errors. The error is calculated as the difference between the measured concentration and its estimate (De Fouquet et al. 2004). The MAE is a measure of the sum of the residuals.

$$MAE = \frac{1}{N} \left[\sum_{i=1}^N Z(x_i) - \hat{Z}(x_i) \right] \tag{6}$$

where \hat{Z} is the predicted value at location i . Smaller MAE values indicate less error. However, the MAE measurement, does not reveal the magnitude of the error that can occur at any point:

$$MSE = \frac{1}{N} \sum_{i=1}^N [Z(x_i) - \hat{Z}(x_i)]^2 \tag{7}$$

The squared elevation of the difference at any point gives an indication of the magnitude, e.g. the smaller the MSE values the more precise the point-by-point estimate. The effectiveness of the prediction compared to that which could have been obtained using the sample mean is given by the measure of G, (Schloeder et al. 2001; Reza et al. 2018).

$$G = \left[1 - \frac{\sum_{i=1}^N [Z(x_i) - \hat{Z}(x_i)]^2}{\sum_{i=1}^N [Z(x_i) - \bar{Z}]^2} \right] \times 100 \tag{8}$$

where \bar{Z} is the sample mean. G is one of the methods used for the accuracy of interpolated maps. (Tsfahunegn et al. 2011). G values are used to check the reliability of the interpolated maps of the concentrations of the studied soil properties. Positive G values indicate that the map obtained by interpolating data from the samples is more accurate than an average. Negative and close-to-zero G values indicate that the average predicts the values at unsampled locations

as accurately as or even better than the sampling estimates (Parfitt et al. 2009).

Results

Statistical analysis

The spatial variation and descriptive statistics of the studied parameters are presented in Fig. 1 and Table 1

Spatial variation of physicochemical parameters

In Table 1, the soil pH in the study area was acidic to near neutral (5.01–6.19), with an average value of 5.58. EC values ranged from 7 to 47 $\mu\text{S}/\text{cm}$, with a mean value of 20.94 $\mu\text{S}/\text{cm}$.

Spatial variation of trace metals

The concentrations of Pb and As ranged from 0.00 to 53.27 mg kg^{-1} and 0.00 to 46.583 mg kg^{-1} , with a mean concentration of 6.17 and 6.01 respectively. The concentrations of Cr, Cu and Ni ranged from 22.15 to 442.44 mg kg^{-1} , 9.25 to 360.37 mg kg^{-1} , and 1.28 to 320.86 mg kg^{-1} , with a mean concentration of 122.1, 169.41, and 192.07 respectively. The CV, was low for all variables, except for Pb and As and the highest CV were observed for Pb (1.95) and As (1.78), while the lowest CV for Cu (0.37). The concentrations of trace metals in the soil decreased in the following order: $\text{Cr} > \text{Ni} > \text{Cu} > \text{Pb} > \text{As}$.

Histograms

The distribution of data sets (histograms) is presented in Fig. 2.

In Fig. 2, the data's histograms revealed that the various parameters were distributed in a skewed unimodal fashion.

In order to comprehend the distribution of the data, a transformation was typically used because the data were severely skewed. The issue of zero concentration values of the components Pb and As was resolved by using a decimal log transformation and adding the constant 1.

Geostatistical modeling

Variographic analysis

The interest of geostatistic consists in particular in taking into account the spatial continuity (structure) of the variable that one wishes to map. Figure 3 shows the spatial distribution of the parameters studied as a function of their concentrations. The characteristics of the semivariogram models shown in Fig. 4 are listed in Table 2. These characteristics make it possible to analyze the spatial variability of the studied parameters; in particular, the thresholds, the RMSE, the nugget effect's amplitude, the ranges, and ultimately the nugget/sill ratio are given careful consideration. The ranges (distances of spatial dependence) of studied parameters were 236.58, 321.78, 396.66, 327.06, 739.55, 271.80, 297.02 m for pH, EC, Cr, Ni, Cu, As and Pb, respectively. Two variogram models were fitted, the exponential model for Ni and Cu with the lowest RMSEs of 1.34 and 2.28, respectively and the spherical model for pH, EC, Cr, As and Pb, with the lowest RMSEs of 0.27, 15.52, 1.27, 17.88 and 12.33, respectively.

Figure 4 shows the experimental variogram of the studied parameters.

The characteristics of the variograms is presented in Table 2.

Cross-validation

The cross-validation results are shown in Table 3 and Fig. 5.

The performance of the ordinary kriging methods was determined by cross-validation using, MSE and MAE. The

Table 1 Descriptive statistics for selected chemical soil parameters

Variable	Standard*	WHO **	Ns	Mean	Med	Min	Max	Skeweness	σ	σ/Mean
pH	–	–	89	5.58	5.56	5.01	6.19	0.11	0.25	0.45
EC ($\mu\text{S}/\text{cm}$)	–	–	89	20.94	18	7	47	0.85	9.29	0.44
Cr mg/kg	120	150	89	122.1	90.67	22.15	442.44	2.01	86.86	0.71
Ni mg/kg	90	90	89	169.41	167.49	9.25	360.37	0.01	90.80	0.53
Cu mg/kg	100	30	89	192.07	207.25	1.28	320.86	– 1.17	71.78	0.37
As mg/kg	18	22	89	6.01	0	0	46.58	1.86	10.73	1.78
Pb mg/kg	140	23	89	6.17	0	0	53.27	2.41	12.10	1.95

Ns number of samples, *min* minimum, *max* maximum, *Med* median, σ standard deviation, σ/Mean coefficient of variation

*AFNOR U 44-041 standard (Villanneau et al. 2008)

**Goria et al. (2010)

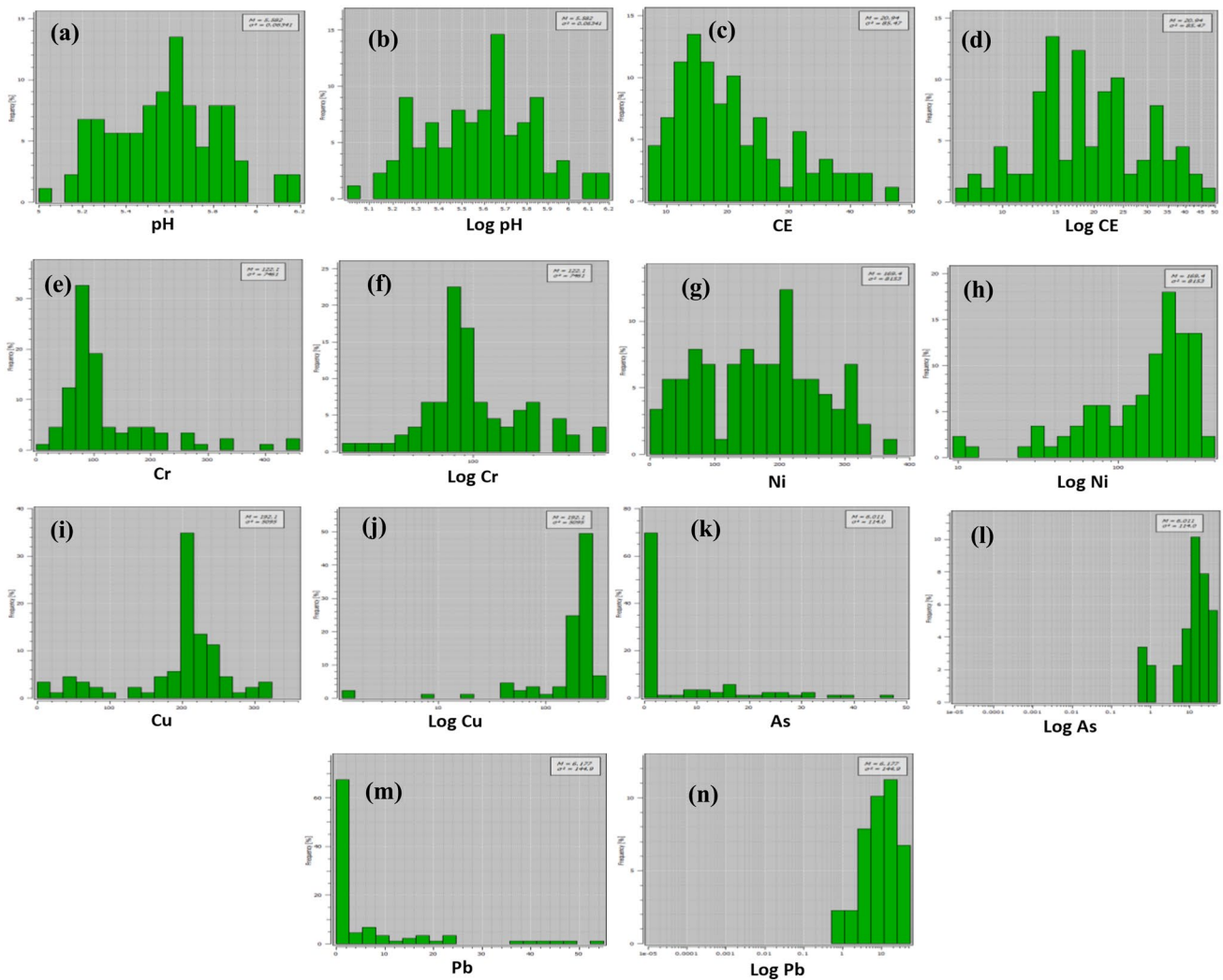


Fig. 2 Histograms of studied parameters: **a** pH; **b** Log pH; **c** EC; **d** Log EC; **e** Cr; **f** Log (Cr); **g** Ni; **h** Log Ni; **i** Cu; **j** Log Cu; **k** As; **l** Log As; **m** Pb and **n** Log10 Pb

ordinary kriging methods were validated at each sample site by nearby samples using the cross-validation technique developed for testing the variogram model, which then compares approximations with actual values.

Kriged interpolation

Ordinary kriging interpolation was used in this study to obtain the prediction maps. Figure 6 and 7 showed respectively the spatial distribution of physicochemical parameters (pH and EC) and the distribution of trace metals (Cr, Ni, Cu, As and Pb) using ordinary kriging interpolation. In Fig. 6, pH values ranged from 5.40 to 5.90, and the predict values of EC ranged from 15.81 to 31.72 μ S/cm. According to trace metals, the range of variation obtained with ordinary

kriging interpolation are 70.55–231.31, 40.65–295.12, 24.03–306.57, 2.56–39.14, 0.10–19.45 mg/kg.

The pH ranged from 5.55 to 5.70 (Fig. 6a).

Discussion

Physicochemical parameter pH and EC concentration in soil

The stability of the soil pH leads to the stability of the dissolved trace metal fractions, an increase leads to their decrease (Ciesielski et al. 2007). The EC varies with the concentration of dissolved salts (Bohn et al. 1985). The high EC and pH generally increases with the salt concentration (Seatz and Peterson 1965). In addition, soil EC could be related to other soil properties such as

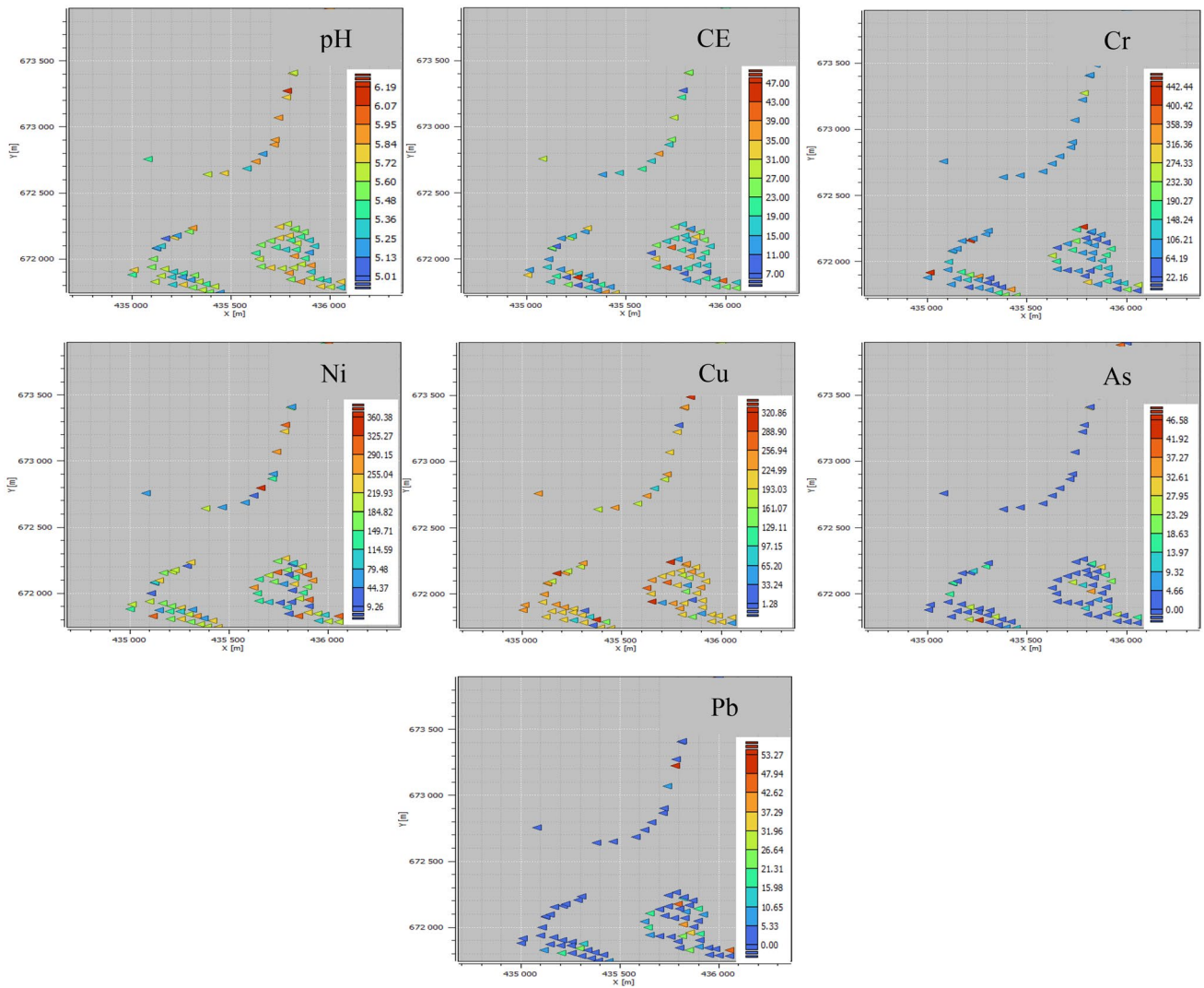


Fig. 3 Sampling points

Table 2 Characteristics of variogram models of studied parameters

Variable	Model	Variance experimental	Nugget effect	Sill	Range (m)	Nugget/sill	RMSE ^a
pH	Spherical	0.06	0.03	0.46	236.58	0.65	0.27
EC	Spherical	85.47	61.75	91.16	321.78	0.67	15.52
Cr	Spherical	7461.61	5491.66	8755.46	396.66	0.62	1.27
Ni	Exponential	8152.60	2319.37	8305.25	327.06	0.27	1.34
Cu	Exponential	5094.50	427.53	5100.18	739.55	0.06	2.28
As	Spherical	114.02	80.48	139.52	271.80	0.57	17.88
Pb	Spherical	144.94	2.38	119.34	297.02	0.27	12.33

^aRoot-mean-square error

water holding capacity, depth of soil humus cover. The pH values observed across the site indicated an acidic pH (5.58–6.19). This low pH may be a sign of acid mine

drainage (AMD) and could be caused, in part, by pyrite (FeS₂) alteration that was observed at the gold mining site. According to the EC values observed in Table 1, all

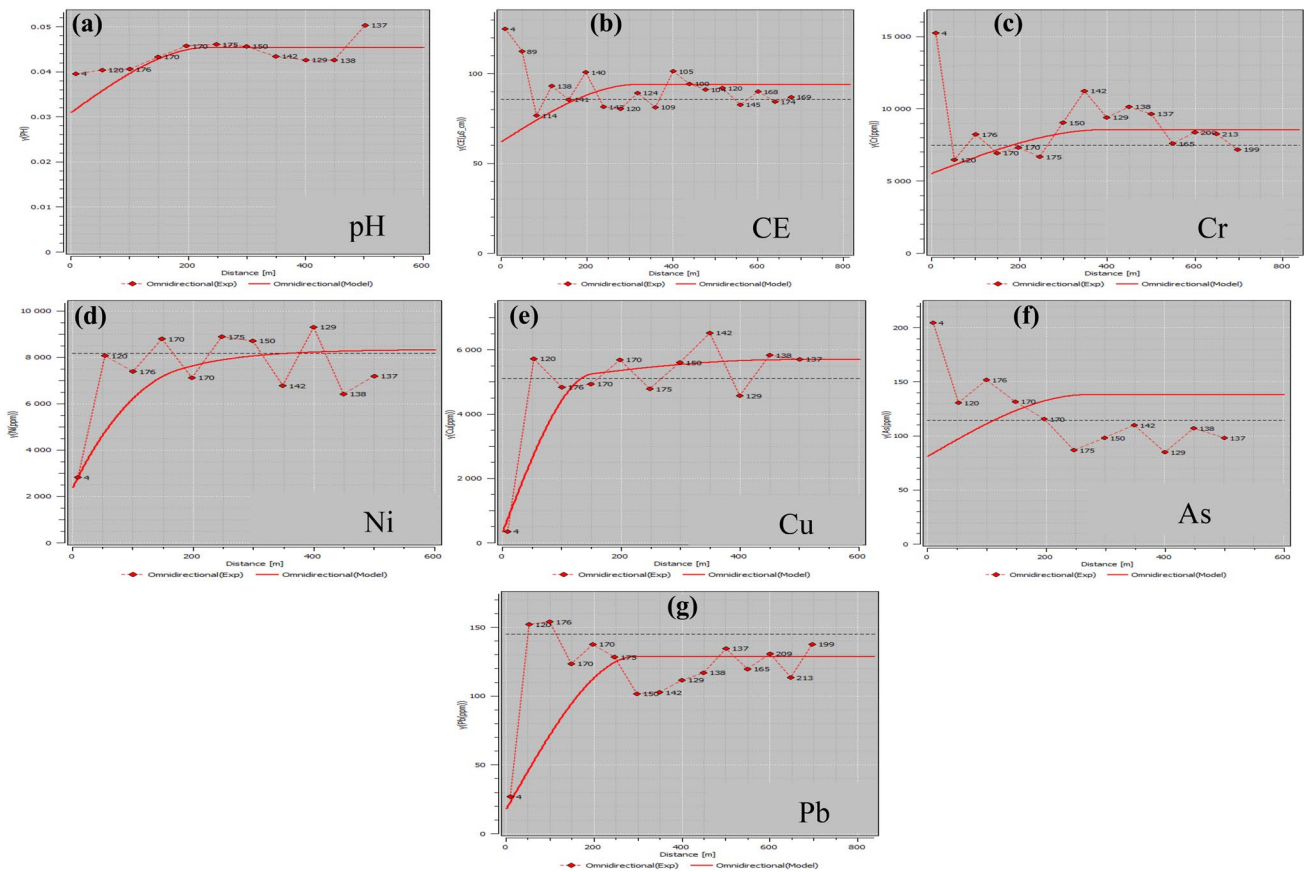


Fig. 4 Omnidirectional variograms of the concentrations and their adjustments: **a** pH; **b** EC; **c** Cr; **d** Ni; **e** Cu; **f** As and **g** Pb

Table 3 Statistics of the cross validation errors

Variables	Mean absolute error	Mean-square error	Goodness of prediction
pH	0.003	1.02	51
EC	0.02	240.9	16
Cr	0.04	11.62	43
Ni	0.04	12.79	41
Cu	0.03	4.69	35
As	0.06	2.19	38
Pb	0.005	2.26	29

the sampled points had low EC values. The EC is conditioned by the geological composition of the study area and varies from medium to high in areas where dolomites predominate (Iavazzo et al. 2012). For pH and EC, Table 1 displays lower values for skewness. This may be related to the inherent properties of variables, mining operations, sampling strategies, and sampling size.

Trace elements in soil

Soil acidity favours the mobility of trace metals Cr, Ni, Cu, As and Pb, notably by dissolving metal salts or destroying the retention phase (Serpaud et al. 1994; Lion 2004). Wide variations in As and Pb displayed values from extremely low to zero that might be regarded as outliers. These abnormally low soil test results could represent a natural or management-induced variance in the study area's soils rather than always being an outlier. Therefore, the presence of outliers in the dataset can alter the structure and characteristics of the variogram. According to Barnett and Lewis (1994), outliers can lead to a phase shift that defies geostatistical theory and cause the variogram to be irregular (Armstrong and Boufassa 1988). To prevent outliers from having a negative impact on the variograms, the outliers for soil Pb and As were changed to the value 1. A number less than 1 implies that the data are distributed normally, and the skewness parameter shows the data's divergence from normalcy (Reza et al. 2018). Considering using a logarithmic transformation was done for skewness coefficients greater than 1 (Webster and Oliver 2008). As and Pb had high skewness values compared

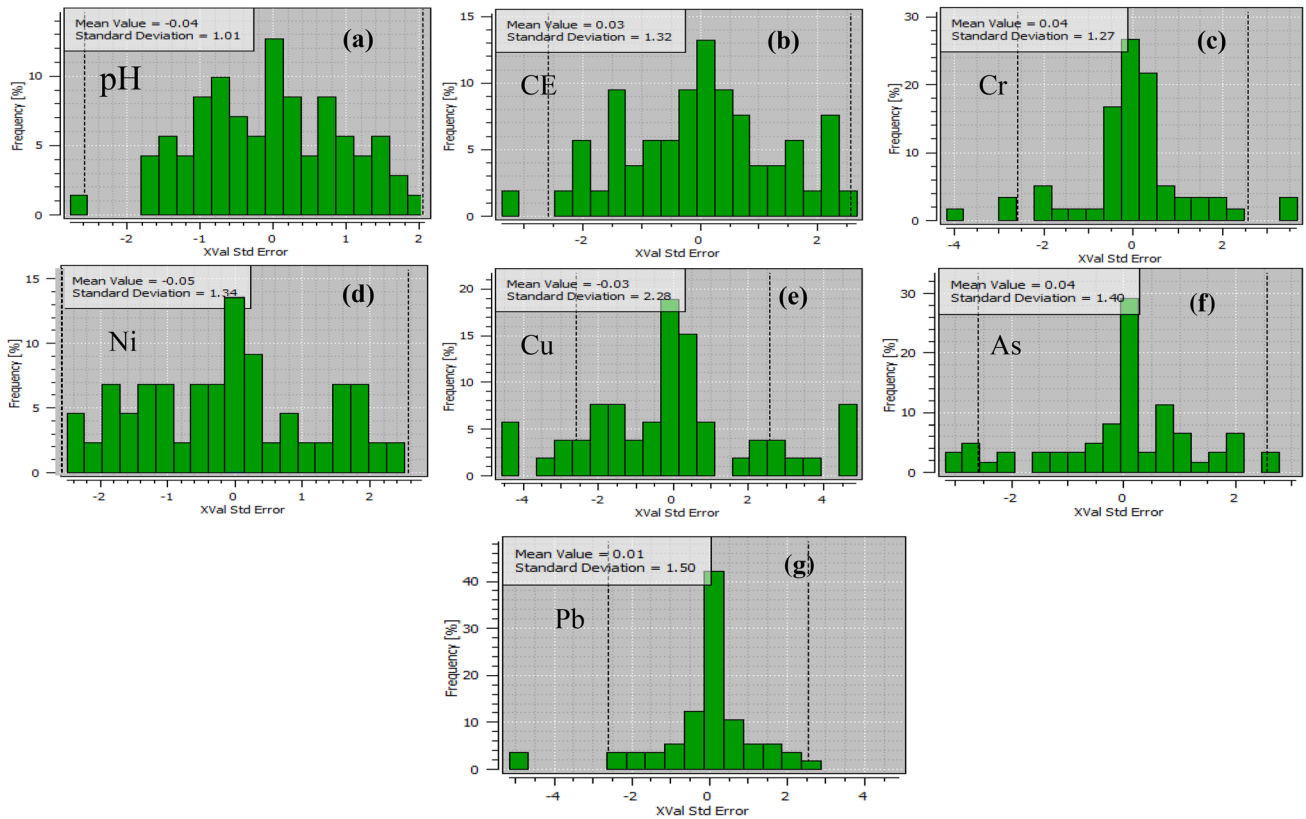


Fig. 5 Histogram of the errors of cross validation

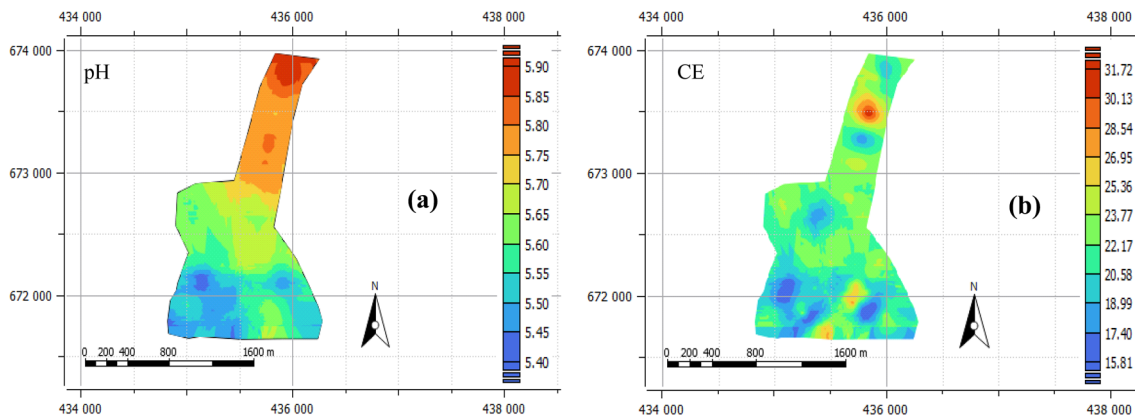


Fig. 6 Kriged maps of physicochemical parameters: **a** pH; **b** EC

to the others (Table 1), which proves that they are irregularly distributed. Various sources of contamination could be responsible for this anomalous distribution. Additionally, the median of each soil attribute was lower than the mean, showing that the sample value was not significantly affected by the anomalous data (Brejda et al. 2000; Cambardella et al. 1994; Cambardella and Karlen 1999; Durdevic et al. 2019; Emadi et al. 2008; Young et al. 1999). With the exception of Pb and As, all soil characteristics

had relatively modest standard deviations when compared to their mean values. This might be explained by the fact that the data range contains a lot of zero values.

The highest and lowest Cr concentrations were observed at sampling points S11 and S16 respectively (Fig. 7a). The majority of the sampling points showed values above the WHO recommended value, implying that the soils at the gold mining site were contaminated with Cr.

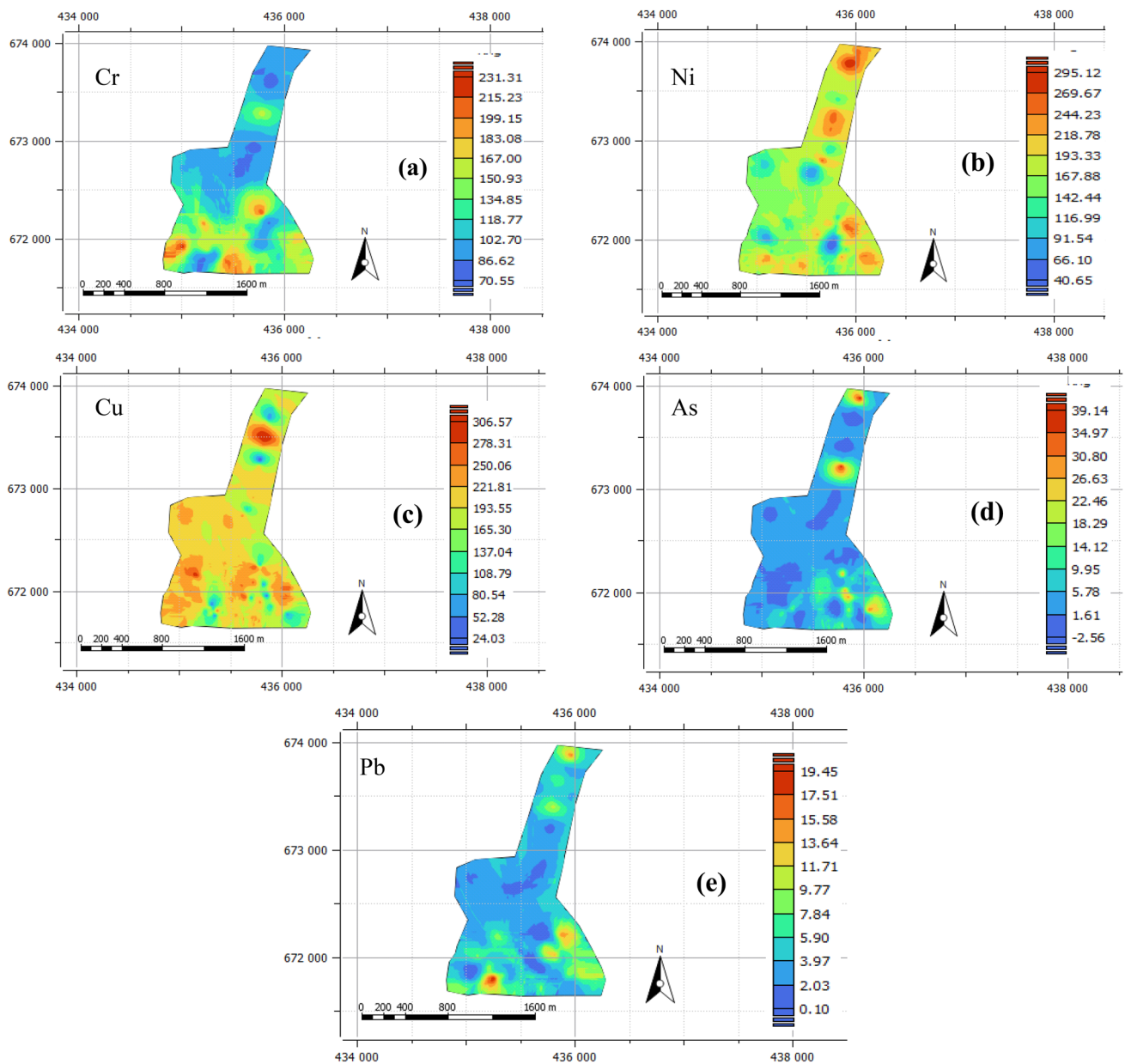


Fig. 7 Kriged maps of **a** Cr; **b** Ni; **c** Cu; **d** As and **e** Pb

In Fig. 7b, sample points E19 and E05 had the highest and lowest Ni concentrations, respectively. E05 was located upstream of the gold mining site, and E19 was a sampling point in the gold mining area. According to the SQG, Ni concentrations were higher than those set by WHO guidelines and AFNOR U 44-041. This shows that the soils at the site were contaminated with Ni. The slow percolation of water through the soil allowing the chlorite to dissolve may be the cause of the high Ni concentrations in the soil.

Low concentrations of Cu were found upstream of the site, while concentrations above the AFNOR U 44-041 standard and WHO guidelines were found in the gold mining

area. Sample points S09 and S23 had the highest and lowest Cu concentrations, respectively (Fig. 7c). Mineral weathering and soil leaching favour high Cu concentrations. Copper is found in abundant and reasonable amounts in the earth's crust (Wedepohl 1995).

The average concentrations of the trace metals Cr, Ni and Cu were higher (Table 1) than those recommended by the World Health Organisation WHO (Goria et al. 2010) and the AFNOR U 44-041 standard (Villanneau et al. 2008). These results indicated, according to the SQG, that the soil was polluted by Cr, Ni and Cu.

As a result, for concentrations like Cr, Cu, Pb, and As, there was a clear distinction between the readability of the concentration and log histograms. The distribution of the pH, EC, and trace metal histograms was favorably skewed.

Spatial variability of pH, EC and trace metals

The variogram (Fig. 4) describes the spatial continuity and regularity of the phenomenon (Webster and Olivier 2006). The numbers indicated the number of pairs of points for each stage of the experimental variogram. The variograms were fitted with the model as well as the parameters nugget effect, sill and range. The isotropic variograms were chosen since the anisotropic variograms did not demonstrate variations in the spatial dependence on direction. While Ni and Cu displayed an exponential pattern, pH, EC, Cr, As, and Pb displayed a spherical pattern. All of the parameter variograms displayed a nugget effect. The variogram threshold is a measure of the values' dispersion and is less susceptible to the size of the field and the asymmetry of the experimental variance data (Matheron 1970).

When compared to the size of the study area, the various indicators indicated a medium range of structure. This structuring indicated minimal variability at close distances and stationarity at this scale. In contrast to the regular variation of the concentrations of the various parameters, the variance of the ranges was minimal throughout the whole study area. The division that was adopted limits the fluctuation in the geographical structure of the concentrations and enables the best possible monitoring of their behavior across the whole study area.

There was a significant discrepancy between the nugget effect values of trace metals and physico-chemical parameters, as shown by the nugget effect values (Table 2), including at least two sources of variability. The sampling error (collection, handling, and measurement), spatial variability for distances below the minimum distances between experimental points, and random and intrinsic variability are likely to blame for the positive nugget seen in all the analyzed parameters (De Fouquet et al. 2004).

The classification of the spatial dependence of the soil properties was done by the nugget/sill ratio. According to Cambardella et al. (1994), the nugget/sill ratio are classified into three classes: Strong (< 25%); Moderate (25–75%) and Random (> 75%). The nugget/sill ratio showed a strong spatial autocorrelation for Cu (0.06), a moderate autocorrelation for pH, EC, Cr, Ni, As and Pb with values of 0.65, 0.67, 0.62, 0.27, 0.57 and 0.27 respectively. Strong and moderate autocorrelation of trace metals and physico-chemical parameters could be attributed to human activities, soil formations and other

external factors such as erosion, leaching. The nugget/sill ratio has suggested that structural factors, such as climate, topography and other natural factors, play an important role in spatial variability (Venteris et al. 2014).

Cross-validation

The results of Fig. 5 and Table 3 revealed that while EC, Cr, Ni, and Cu had relatively high MAEs and MSEs, pH, As, and Pb had relatively low MAEs and MSEs. The G-values were greater than 0 for all the variables, demonstrating that using the variogram parameters for spatial prediction was preferable than assuming that each unsampled location's property value would equal the average of the observed value. This shows that the variogram parameters that were created by fitting the experimental variogram values were enough for representing the spatial variation of pH, EC, Cr, Ni, Cu, As, and Pb. Cross-validation findings verified that the variogram parameters created by fitting the experimental variogram values were accurate and consistent.

Interpolation maps

These acidic pH levels may be the result of mining operations and the beginning of acid mine drainage. The northern part of the study area was where the low pH was most prevalent. The EC prediction map (Fig. 6b) revealed that soil salinity was at its lowest in the study area's western portion and at its highest in the study area's northern (low elevation) and majority of center part. Variations in erosion instability, water runoff, and micro-topography may be responsible for this greatest capacity for change over short distances (Behera and Shukla 2015).

High concentrations were observed on the Cr prediction map (Fig. 7a) in the part area's south and southwest. Slight Cr concentrations were found in the center of the study area, and these concentrations moved eastward. The Ni prediction map (Fig. 7b) displayed an uneven distribution of Ni concentrations throughout the whole study area. In the northern part of the study area, there were high Ni concentrations found. According to the Cu prediction map (Fig. 7c), Cu concentrations were seen practically everywhere in the area, with the highest concentrations found in the northern, southern, and eastern regions. Significant As concentrations were found to the north and south-east of the study area (Fig. 7d). Finally, the Pb prediction map (Fig. 7e) displayed average Pb concentrations in the study area's north and east. Mining activities with the extraction works that promote the natural weathering of trace metals in the surrounding rocks and minerals of the study region can be considered the primary cause of pollution.

Conclusions

This paper investigated the spatial variability of pH, EC and trace metals in the soils of the abandoned mining district of Bindiba (East Cameroon) using geostatistical approach. The soils of the mining area were acidic to near neutral, slightly conductible and polluted by trace metals. The variographic analysis revealed that the spatial variability was described by the spherical model for pH, EC, Cr, As and Pb and the exponential model for Ni and Cu. The high spatial dependence of pH, EC and trace metals was observed as a considerable autocorrelation between the variables indicating that these trace metals were controlled by external factors such as mining activity, rocks and minerals weathering and internal factors such as soil composition. Cross-validation was used to choose variogram models for basic kriging, which made it possible to create accurate maps of pH, EC, and trace metal concentrations in un-sampled locations. According to the modeling of the spatial structure, The nugget/sill ratio showed a strong spatial autocorrelation for Cu (nugget/sill ratio < 25%), and moderate autocorrelation for pH, EC, Cr, Ni, As and Pb (nugget/sill ratio 25–75%). Therefore, compared to direct measurement, which involves time and costs, the geostatistical approach to assessing soil contamination in un-sampled locations appears to be a precise and reliable tool for accurate prediction. It could also help in decision-making for developing a better strategy for remediating abandoned mining sites.

Acknowledgements The authors would like to thank Geovariances Company for providing ISATIS.neo licence. Authors are grateful to the Framework of Support for the Promotion of Mining Handicrafts “(CAPAM)” laboratory for their support during the analysis works. The authors are also grateful to Eco-materials and Environment Laboratory of the School of Geology and Mining Engineering, University of Ngaoundere.

Funding This research did not receive any specific grant from funding agencies in the public, commercial, or not-for-profit sectors.

Availability of data and materials The datasets used and/or analyzed during the current study are available from the corresponding author on reasonable request.

Declarations

Conflict of interest On behalf of all authors, the corresponding author states that there is no conflict of interest.

References

Alloway BJ, Ayres DC (1997) Chemical principles of environmental pollution. Black Academic and Professional, an imprint of Chapman and Hall, London, p 394

- Armstrong M, Boufassa A (1988) Comparing the robustness of ordinary kriging and lognormal kriging: outlier resistance. *Math Geol* 20:447–457
- Austruy A (2012) Aspects physiologiques et biochimiques de la tolérance à l'arsenic chez les plantes supérieures dans un contexte de phytostabilisation d'une friche industrielle. In: Thèse. Université Blaise Pascal, Clermont-Ferrand, p 300
- Ayiwouo MN, Mambou LL, Boroh WA, Sifeu KT, Ngounouno I (2022) Spatial variability of trace metals in sediment along the Lom River in the gold mining area of Gankombol (Adamawa Cameroon) using geostatistical modeling methods. *Model Earth Syst Environ*. <https://doi.org/10.1007/s40808-022-01500-9>
- Baillargeon S (2005) Le Krigeage: In revue de la théorie et application à l'interpolation spatiale de données de précipitations, Thèse et mémoires. Université de Laval, p 8
- Baize (2009) Element trace dans le sol. Fonds géochimiques, fonds pédogéochimiques naturels en teneurs agricoles habituelles: définition et utilités. *Courrier de l'environnement* 57:63–72
- Barnett V, Lewis T (1994) Outliers in statistical data. Wiley, New York
- Behera S, Shukla A (2015) Spatial distribution of surface soil acidity, electrical conductivity, soil organic carbon content and exchangeable Potassium, calcium and magnesium in some cropped acid Soils of India. *Land Degrad Dev* 26:71–79
- Behera SK, Suresh K, Rao BN, Mathur RK, Shukla AK, Manorama K, Ramachandrudu K, Harinarayana P, Prakash C (2016) Spatial variability of some soil properties varies in oil palm (*Elaeis guineensis* Jacq.) plantations of west coastal area of India. *Solid Earth* 7(3):979–993
- Belkessam L, Lemiere B (2006) Stratégie et Technique d'échantillonnage des sols pour l'évaluation des pollutions. RECORD Rapport final, CNRSSP, 321p, n°04–0510/1A
- Bhunia GS, Shitb PK, Chattopadhyay R (2018) Assessment of spatial variability of soil properties using geostatistical approach of lateritic soil (West Bengal, India). *Ann Agrarian Sci* 16:436–443
- Bobbia M, Pernelet V, Ch R (2001) L'intégration des informations indirectes à la cartographie géostatistique des polluants. In: pollution Atmosphérique, avril-juin 170:251–261
- Bohn H, McNeal B (1985) Soil Chemistry, 2nd edn. Wiley, New York
- Brejda J, Moorman T, Smith J, Karlen D, Allan D, Dao T (2000) Distribution and variability of surface soil properties at a regional scale. *Soil Sci Soc Am J* 64:974–982
- Cambardella C, Karlen D (1999) Spatial analysis of soil fertility parameters, precision. *Agriculture* 1:5–14. <https://doi.org/10.1023/A:10025919134>
- Cambardella C, Moorman T, Novak J, Parkin T, Karlen D, Konopka A (1994) Field scale variability of soil properties in central Iowa soil. *Soil Sci Soc Am J* 58:1501–1511. <https://doi.org/10.2136/sssaj1994.03615995005800050033x>
- Chambers RL, Yarus JM, Kirk BH (2000) Petroleum geostatistics for nongeostatisticians. *Lead Edge* 19:474–479
- Chen Z, Huang S, Chen L, Cheng B, Li M, Huang H (2021) Distribution, source, and ecological risk assessment of potentially toxic elements in surface sediments from Qingfeng River, Hunan, China. *J Soils Sediments* 21:2686–2698
- Chiles JP, Delfiner P (2009) Geostatistics: modeling spatial uncertainty. Wiley
- Chiles J, Delfiner P (1999) Geostatistics: modeling spatial uncertainty. In: Wiley series in probability and statistics: applied probability and statistics section. Wiley, New York
- Ciesielski A (2007) Effets du pH sur l'extraction des éléments traces métalliques dans les sols. *Etude Gestion Des Sols* 1(14):24
- Custer K (2003) Cleaning up Western watersheds. Mineral Policy Center, Boulder
- de Fouquet C (2004) Estimation de la concentration en hydrocarbures totaux du sol d'un ancien site pétrochimique: étude méthodologique. *Oil Gas Sci Technol Rev* 59(3):275–295

- Davis BM (1987) Uses and abuses of cross-validation in geostatistics. *Math Geol* 19:241–324
- Delfiner P (1976) Linear estimation of non stationary spatial phenomena. *Advanced geostatistics in the mining industry*
- Demougeot RH, Haouche-Belkessam L, Denis S, Garcia M (2008) Reconnaissance assistée de sites pollués par l'utilisation conjointe de mesures rapides sur site et de traitements géostatistiques-partie 2. Conception et validation d'une démarche itérative de reconnaissance. Rapport final REPERAGE. Rapport FSSADEME2007002
- Demougeot RH, Haouche-Belkessam L, Denys S, Garcia M, D'Or D (2009) Couplage de mesures sur site et de méthodes géostatistiques: mise en oeuvre "en temps réel" à l'aide d'un FPXRF. *Projet REPERAGE. 2. Rencontres nationales de la recherche sur les sites et sols pollués. ADEME Edition. Anger, Paris*, pp NC
- Deraisme J, Bobbia M (2003) L'apport de la géostatistique à l'étude des risques liés à la pollution atmosphérique. *Environ Risque Santé* 2:168–175
- Dère (2006) Mobilité et redistribution à long terme des éléments traces métalliques exogènes dans les sols. Institut National d'agronomie, Paris-Grignon
- Durdevic B, Jug I, Jug D et al (2019) Spatial variability of soil organic matter content in eastern Croatia assessed using different interpolation methods. *Int Agrophys* 33(1)
- Edraki M, Yun (2005) Hydrochemistry, mineralogy and sulfure isotope geochemistry of acide mine drainage at the Mt. In: *Applied geochemistry. Morgan mine environment, Queensland*, pp 785–805
- Emadi M, Baghernejad M, Emadi M, Maftoun M (2008) Assessment of some properties by spatial variability in saline and sodic soils in Arsanjan plain Sourthen Iran. *Pak J Biol Sci* 2(11):238–243. <https://doi.org/10.3923/pjbs.2008.238-243>
- Florine G, Christian C, Garcia MH, Jean-Baptiste Mathieu JD (2019) Approche géostatistique appliquée à l'évaluation d'un état de pollution des sols dans le cadre d'une session de site industriel. KIDOVA, France
- Gaida TC, Snellen M, Thaienne AGP, Dijk V, Dick GS (2019) Geostatistical modelling of multibeam backscatter for fullcoverage seabed sediment maps. *Hydrobiologia* 845:55–79
- Garcia F, Mathieu JB, Garcia M (2019) Suite d'outils logiciels pour la conduite de campagnes de reconnaissance de sites potentiellement pollués couplant mesures sur site et traitement géostatistique des données. Communication soumise aux rencontres de la Recherche sur les sites et sols pollués
- GeoSiPol (2005) Géostatistique appliquée aux sites et sols pollués. Manuel méthodologique et exemple d'application, p 139
- Goodchild MF, Parks BO, Steyaret LT (1993) *Environmental modelling with GIS*. Oxford University Press, New York
- Goria S, Stempfhelet M, de Crouy-Chanel P (2010) Introduction aux statistiques spatiales et aux systèmes d'information géographiques en santé environnement. Application aux études écologiques, Département santé environnement, Institut de veille sanitaire, p 4
- Gouzy A, Ducos G (2008) La connaissance des éléments traces métalliques: un défi pour la gestion de l'environnement. In: *Air pur*, pp 6–10
- Gy P (1988) Hétérogénéité, échantillonnage, homogénéisation. Ensemble cohérent de théorie. In: Masson (ed) *Sciences de l'ingénieur-collection Mesures Physiques*, Paris, p 608
- IAEA (2004) *Soil sampling for environmental contaminants. Rapport IAEA-TECDOC-1415*
- Jaishankar TT (2014) Toxicity, mechanism and health effects of some heavy metals. *Interdiscip Toxicol* 60–72
- Jaishankar M, Tsenten T, Anbalanga N (2014) Toxicity mechanism and health effects of some heavy metals. *Interdiscip. Toxicol.* 7(2):60–72
- Jeannée N (2005) National cartography of the pollution by NO₂ and PM₁₀ in France—contrat ADEME 0362 C0023 et 0362 C0053. Rapport final, décembre 2003. Mise à jour: cartographie nationale NO₂ et PM₁₀: état en 2000 et projection en 2010, par attribuable au trafic et exposition des populations -note technique finale, avril 2005
- Jeannée N, de Fouquet C (2000) Characterization of soil pollutions from former coal processing site. In: Kleigeld W, Krige D (eds) *Geostats*. Sous presse
- Jeannée N, de Fouquet C (2003) Apport d'informations qualitatives pour l'estimation des teneurs en milieux hétérogènes: cas d'une pollution de sols par des hydrocarbures aromatiques polycycliques (HAP). *Comptes Rendus Géoscience* 335(5):441–449
- Journel AG, Huijbregts CJ (1978) *Mining Geostatistics*. Academic Press Inc, London
- Jung M (2001) Heavy metal contamination of soil and water in and around the Imcheon Au-Ag mine. *Korea Appl Geochem* 16:1369–1375
- Khan M, Amin MS, Bhuiyan MMR (2019) Spatial variability and geostatistical analysis of selected soil Bangladesh. *J Sci Ind Res* 1(54):55–56
- Kumar S, Vo AD, Qin F, Li H (2016) Comparative assessment of methods for the fusion transcripts detection from RNA-Seq data. *Sci Rep* 6(1):1–10
- Leenaers H, Okx JP, Burrough P (1989) Co-kriging: an accurate and inexpensive means of mapping floodplain soil pollution by using elevation data. In: Armstrong M (ed) *Geostatistics*. Kluwer, Dordrecht, pp 371–382
- Lion J (2004) Etude hydrogéochimique de la mobilité de polluants inorganiques dans sédiments de curage mis en dépôt: expérimentations, études in situ et modélisation. In: Thèse doctorat. Ecole Nationale Supérieure des Mines de Paris France, Paris, p 248
- Liu CL, Wu YZ, Lui QJ (2015) Effects of land use on spatial patterns of soil properties in a rocky mountain area of Northern China. *Arab J Geosci* 8:1181–1194
- Lottermoser B, Ashley AP (2005) Tailing dam seepage at the rehabilitated Mary Kathleen uranium mine, Australia. *J Geochem Explor*
- Malherbe L, Rouil L (2003) Méthodes de représentation de la qualité de l'air. Guide D'utilisation Des Méthodes De La Géostatistique Linéaire, Décembre 2003:22
- Matheron G (1970) La théorie des variables régionalisées, et ses applications. Cahiers du CMM, fascicule 5. Ecole des mines de Paris, Paris
- Mathieu J, Kaskassian S, Garcia M (2014) Apport de la géostatistique au diagnostic de sites et sols pollués: prolongement d'un cas d'étude de démonstration GeoSiPol. 3ème Rencontres nationales de la recherche sur les sites & sols pollués, 18 au 19 novembre 2014. Paris, France
- Pansu M, Gautheyrou J (2006) *Handbook of soil analysis*. Springer-Verlag, Berlin
- Parfitt RL, Mackay AD, Ross DJ, Budding PJ (2009) Effects of soil fertility on leaching losses of N, P and C in hill country. *N Z J Agric Res* 52(1):69–80
- Parker HM, Journel AG, Dixon WC (1979) The use of conditional lognormal probability distribution for the estimation of open-pit ore reserves in stratabound uranium deposits a case study. Proceedings of the 16th APCOM international
- Reza SK, Dutta D, Bandyopadhyay S, Singh SK (2018) Spatial variability analysis of soil properties of Tinsukia District, Assam. *India Natl Acad Agric Sci* 8(2):231–238
- Rivoirard J (2003) Cours de géostatistique multivariable, centre de géostatistique. FONTAINEBLEAU Février 2003:10–11
- Schloeder CA, Zimmermen NE, Jacobs MJ (2001) Comparison of methods for interpolating soil properties using limited data. *Soil Sci Soc Am J* 65:470–479

- Scholz M, Olivier M, Webster R, Loveland J, McGrath S (1999) Sampling to monitor soil in England and Wales. In: Gomez-Hernandez J, Soares A, Froidevaux R (eds) *Geostatistics for environmental application*. Kluwer Academic Publishers: geoENV II-Geostatistics for Environmental Application
- Seatz L, Peterson H (1965) Acid, alkaline, saline, and sodic soils. In: *Chemistry of the soil*, Reinhold Pub, New York, pp 292–319
- Serpaud B, AL-Shukry M, Casteigneau M, Matejka G (1994) Adsorption des métaux lourds (Cu, Zn, Cd, et Pb) par les sédiments superficiels d'un cours d'eau: rôle du pH, de la température et de la composition du sédiment. *Revue des sciences de l'eau* 7:343–365
- Shit KP, Bhunia GS, Maiti R (2016) Spatial analysis of soil properties using GIS based geostatistics models. *Model Earth Syst Environ* 2:107. <https://doi.org/10.1007/s40808-016-0160-4>
- Sigg., Stumm, W., & Berha, P. (1992) *Chimie des eaux naturelles et des interfaces dans l'environnement*. Masson, Paris
- Tesfahunegn GB, Tamene L, Vlek PLG (2011) Catchmentscale spatial variability of soil properties and implications on sitespecific soil management in northern Ethiopia. *Soil Tillage Res* 117:124–139
- Tripathi R, Nayak AK, Shahid M, Raja R, Panda BB, Mohanty S, Kumar A, Lal B, Gautam P, Sahoo RN (2015) Characterizing spatial variability of soil properties in salt affected coastal India using geostatistics and kriging. *Arab J Geosci* 8(12):10693–10703
- Utset A, Lopez T, Diaz M (2000) A comparison of soil maps, kriging and a combined method for spatially prediction bulk density and field capacity of ferralsols in the Havana-Matanaz Plain. *Geoderma* 96:199–213
- Venteris EN, Basta J, Bigham RR (2014) Modeling spatial patterns in soil arsenic to estimate natural baseline concentrations. *J Environ Qual* 43(3):936–946
- Veronesi F, Corstanje R, Mayr T (2014) Landscape scale estimation of soil carbon stock using 3D modelling. *Sci Total Environ* 487:578–586
- Verfaillie E, Van Lancker V, Van Meirvenne M (2006) Multivariate geostatistics for the predictive modelling of the surficial sand distribution in shelf areas. *Cont Shelf Res* 26:2454–2468
- Villanneau E, Perry-Giraud, Saby N, Jolivet C, Marot F, Maton D, Floch-Barneaud A, Antoni V, Arrouays D (2008) Détection de valeurs anormales d'éléments traces métalliques dans les sols à l'aide du réseau de mesure de la qualité des sols. 15(3):183
- Waller LA, Carol AG (2004) *Applied spatial statistics for public health data*. Wiley, USA
- Wavrer P (1997) *Méthodologies et stratégie d'échantillonnage de sols*. Rapport CNRSP/1997/11
- Webster R, Oliver MA (2006) *Geostatistics for environmental scientists*. John Wiley & Sons
- Webster R, Oliver MA (2008) *Geostatistics for environmental scientists*, 2nd edn. Wiley, Hoboken, NJ, USA
- Wedepohl HK (1995) The composition of the continental crust. *Geochim Cosmochim Acta* 59:1445–1490
- Wu C, Luo Y, Whang LM (2010) Variability of copper availability in paddy fields in relation to selected soil properties in southeast China. *Geoderma* 156:200–206
- Yasrebi J, Saffari M, Fathi H, Karimian N, Moazallahi M, Gazni R (2009) Evaluation and comparison of ordinary kriging and inverse distance weighting methods for prediction of spatial variability of some soil chemical parameters. *Res J Biol Sci* 4(1):93–102
- Young F, Hammer R, Larsen D (1999) Frequency distributions of soil properties on loessmantled Missouri watershed. *Soil Sci Soc Am J* 63:178–185. <https://doi.org/10.2136/sssaj1999.03615995006300010025x>
- Zhao Z, Yang Q, Benoy G, Chow TL, Xing Z, Rees HW, Meng F-R (2010) Using artificial neural network models to produce soil organic carbon content distribution maps across landscapes. *Can J Soil Sci* 90(1):75–87

Publisher's Note Springer Nature remains neutral with regard to jurisdictional claims in published maps and institutional affiliations.

Springer Nature or its licensor holds exclusive rights to this article under a publishing agreement with the author(s) or other rightsholder(s); author self-archiving of the accepted manuscript version of this article is solely governed by the terms of such publishing agreement and applicable law.